

# SUPPORTING INFORMATION

## Alkylaluminum-Complexed Zirconocene Hydrides – Identification of Hydride-Bridged Species by NMR-Spectroscopy.

Steven M. Baldwin,<sup>†</sup> John E. Bercaw,<sup>\*,†</sup> and Hans H. Brintzinger<sup>\*,‡</sup>

Contribution from the Arnold and Mabel Beckman Laboratories of Chemical Synthesis, California Institute of Technology, Pasadena, California 91125, USA, and Fachbereich Chemie, Universität Konstanz, D-78457 Konstanz, Germany

E-mail: Bercaw@caltech.edu; Hans.Brintzinger@uni-konstanz.de

### NMR Spectra:

- Figure S1.**  $(C_5H_5)_2ZrH_2$  (**3**) + 1 eq  $HAi^iBu_2$  + 1 eq  $ClAl^iBu_2$  S3
- Figure S2.**  $(C_5H_5)_2ZrH_2$  (**3**) + 1 eq  $HAi^iBu_2$  + 2 eq  $ClAl^iBu_2$  S3
- Figure S3.**  $(C_5H_5)_2ZrH_2$  (**3**) + xs  $HAi^iBu_2 \rightarrow (C_5H_5)_2Zr(\mu-H)_3(Al^iBu_2)_3(\mu-H)_3$  (**5**) S4
- Figure S4.**  $(^iBu-Cp)_2ZrCl_2$  (**6**) + 2  $HAi^iBu_2 \rightarrow (^iBu-Cp)_2Zr(\mu-H)_3(Al^iBu_2)_3(\mu-H)_3$  (**7**) S4
- Figure S5.**  $(1,2-Me_2-C_5H_3)_2$  (**8**) + xs  $HAi^iBu_2 \rightarrow (1,2-Me_2-C_5H_3)_2Zr(\mu-H)_3(Al^iBu_2)_3(\mu-H)_3$  (**9**) S5
- Figure S6.**  $(Me_3Si-C_5H_4)_2$  (**10**) + 2  $HAi^iBu_2 \rightarrow (Me_3Si-C_5H_4)_2Zr(\mu-H)_3(Al^iBu_2)_3(\mu-H)_3$  (**11**) S5
- Figure S7.**  $(C_5Me_5)ZrH_2$  (**13**) + 2  $Al^iBu_3 \rightarrow (C_5Me_5)ZrH^iBu$  (**14**) and  $(C_5Me_5)Zr^iBu_2$  (**15**) S6
- Figure S8.**  $(EBI)ZrCl_2$  (**17**) + 2  $HAi^iBu_2 \rightarrow (EBI)ZrCl(\mu-H)_2Al^iBu_2$  S6
- Figure S9.**  $(EBTHI)ZrCl_2$  (**18**) + 2  $HAi^iBu_2 \rightarrow (EBTHI)ZrCl(\mu-H)_2Al^iBu_2$  S7
- Figure S10.**  $Me_2C(C_5H_4)ZrCl_2$  (**19**) + xs  $HAi^iBu_2 \rightarrow Me_2C(C_5H_4)ZrCl(\mu-H)_2Al^iBu_2$  S7
- Figure S11.**  $Me_2Si(C_5H_4)_2ZrCl_2$  (**20**) + 6  $HAi^iBu_2 \rightarrow Me_2Si(C_5H_4)ZrCl(\mu-H)_2Al^iBu_2$  S8
- Figure S12.**  $Me_2Si(2,4-Me_2-C_5H_2)_2ZrCl_2$  (**21**) + xs  $HAi^iBu_2 \rightarrow Me_2Si(2,4-Me_2-C_5H_2)ZrCl(\mu-H)_2Al^iBu_2$  S8
- Figure S13.**  $(Me_2Si)_2(C_5H_3)_2ZrCl_2$  (**22**) + 2  $HAi^iBu_2 \rightarrow (Me_2Si)_2(C_5H_3)ZrCl(\mu-H)_2Al^iBu_2$  S9
- Figure S14.**  $(Me_2Si)_2(2,4-^iPr_2-C_5H)(C_5H_3)ZrCl_2$  (**23**) + 2  $HAi^iBu_2 \rightarrow$   
 $(Me_2Si)_2(2,4-^iPr_2-C_5H)(C_5H_3)ZrCl(\mu-H)_2Al^iBu_2$  S9
- Figure S15.** gCOSY for  $(EBTHI)ZrH(\mu-H)_2Al^iBu_2$  (**25**) S10
- Figure S16.**  $((EBTHI)ZrH_2)_2$  (**24**) + 4  $HAi^iBu_2$  + 2  $ClAl^iBu_2 \rightarrow (EBTHI)ZrCl(\mu-H)_2Al^iBu_2$  S10
- Figure S17.**  $((EBTHI)ZrH_2)_2$  (**24**) + 4  $HAi^iBu_2$  + 4  $ClAl^iBu_2 \rightarrow (EBTHI)ZrCl(\mu-H)_2Al^iBu_2$  S11
- Figure S18.** *rac*- $Me_2C(indenyl)_2ZrCl_2$  (**28**) + 2 eq  $HAi^iBu_2 \rightarrow rac$ - $Me_2C(indenyl)_2ZrCl(\mu-H)_2Al^iBu_2$  S11

- Figure S19.** *meso*-Me<sub>2</sub>C(indenyl)<sub>2</sub>ZrCl<sub>2</sub> (**28**) + 2 eq HAl<sup>*i*</sup>Bu<sub>2</sub> →  
*meso*-Me<sub>2</sub>C(indenyl)<sub>2</sub>ZrCl(μ-H)<sub>2</sub>Al<sup>*i*</sup>Bu<sub>2</sub> S12
- Figure S20.** gCOSY of *rac*-Me<sub>2</sub>Si((2-Me<sub>3</sub>Si-4-Me<sub>3</sub>C-C<sub>5</sub>H<sub>2</sub>)ZrH(μ-H)<sub>2</sub>Al<sup>*i*</sup>Bu<sub>2</sub> (**32**) S12
- Figure S21.** NOE of *rac*-Me<sub>2</sub>Si((2-Me<sub>3</sub>Si-4-Me<sub>3</sub>C-C<sub>5</sub>H<sub>2</sub>)ZrH(μ-H)<sub>2</sub>Al<sup>*i*</sup>Bu<sub>2</sub> (**32**) S13
- Figure S22.** *meso*-Me<sub>2</sub>Si(3-Me<sub>3</sub>C-C<sub>5</sub>H<sub>2</sub>)<sub>2</sub>ZrCl<sub>2</sub> (**33**) + 2 eq HAl<sup>*i*</sup>Bu<sub>2</sub> →  
*meso*-Me<sub>2</sub>Si(3-Me<sub>3</sub>C-C<sub>5</sub>H<sub>2</sub>)<sub>2</sub>ZrCl(μ-H)<sub>2</sub>Al<sup>*i*</sup>Bu<sub>2</sub> (**34**) S14
- Figure S23.** gCOSY of *meso*-Me<sub>2</sub>Si(3-Me<sub>3</sub>C-C<sub>5</sub>H<sub>2</sub>)<sub>2</sub>ZrCl(μ-H)<sub>2</sub>Al<sup>*i*</sup>Bu<sub>2</sub> (**34**) S14
- Figure S24.** NOE of *meso*-Me<sub>2</sub>Si(3-Me<sub>3</sub>C-C<sub>5</sub>H<sub>2</sub>)<sub>2</sub>ZrCl(μ-H)<sub>2</sub>Al<sup>*i*</sup>Bu<sub>2</sub> (**34**) S15
- Figure S25.** H<sub>4</sub>C<sub>2</sub>(C<sub>5</sub>H<sub>4</sub>)<sub>2</sub>ZrCl<sub>2</sub> (**35**) + 4 eq HAl<sup>*i*</sup>Bu<sub>2</sub> → H<sub>4</sub>C<sub>2</sub>(C<sub>5</sub>H<sub>4</sub>)<sub>2</sub>Zr(μ-H)<sub>3</sub>(Al<sup>*i*</sup>Bu<sub>2</sub>)<sub>3</sub>(μ-H)<sub>3</sub> (**37**) S15
- Figure S26.** NOE of Me<sub>4</sub>C<sub>2</sub>(C<sub>5</sub>H<sub>4</sub>)<sub>2</sub>Zr(μ-H)<sub>3</sub>(Al<sup>*i*</sup>Bu<sub>2</sub>)<sub>3</sub>(μ-H)<sub>3</sub> (**38**) S16
- Figure S27.** (EBTHI)ZrF<sub>2</sub> + 1 eq HAl<sup>*i*</sup>Bu<sub>2</sub> → ((EBTHI)ZrH<sub>2</sub>)<sub>2</sub> + (EBTHI)ZrF<sub>2</sub> S16
- Appendix S-1.** Analysis of changes in the chemical shift of the ZrH<sub>2</sub> signal of (SBI)ZrCl(μ-H)<sub>2</sub>Al<sup>*i*</sup>Bu<sub>2</sub> upon addition of Al<sub>2</sub>Me<sub>6</sub>. S17

**Figure S1.**  $^1\text{H}$  spectrum of  $(\text{C}_5\text{H}_5)_2\text{ZrH}_2$  (**3**) with 1 equiv.  $\text{HAl}^i\text{Bu}_2$  and 1 equiv.  $\text{ClAl}^i\text{Bu}_2$  in benzene- $d_6$  at  $25^\circ\text{C}$ .

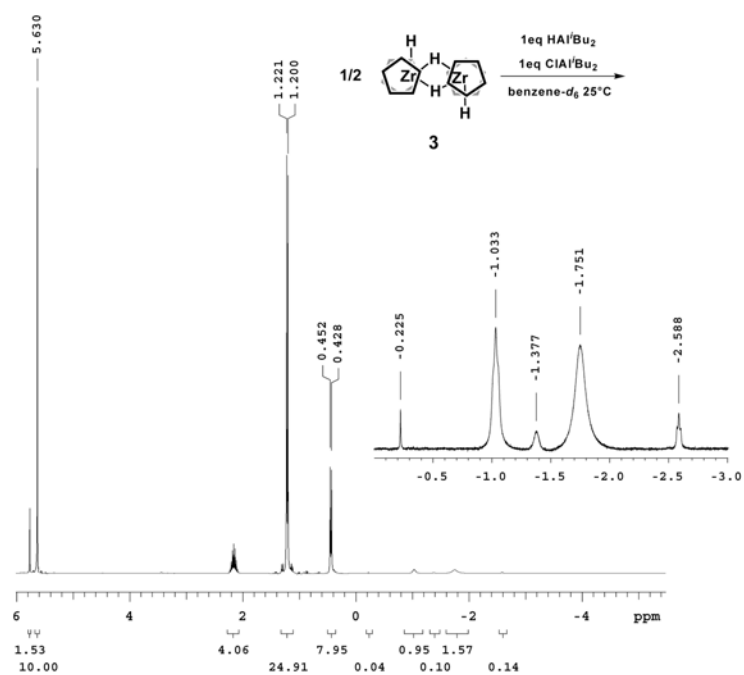


**Figure S2.**  $^1\text{H}$  spectrum of  $(\text{C}_5\text{H}_5)_2\text{ZrH}_2$  (**3**) with 1 equiv.  $\text{HAl}^i\text{Bu}_2$  and 2 equiv.  $\text{ClAl}^i\text{Bu}_2$  in benzene- $d_6$  at  $25^\circ\text{C}$ .

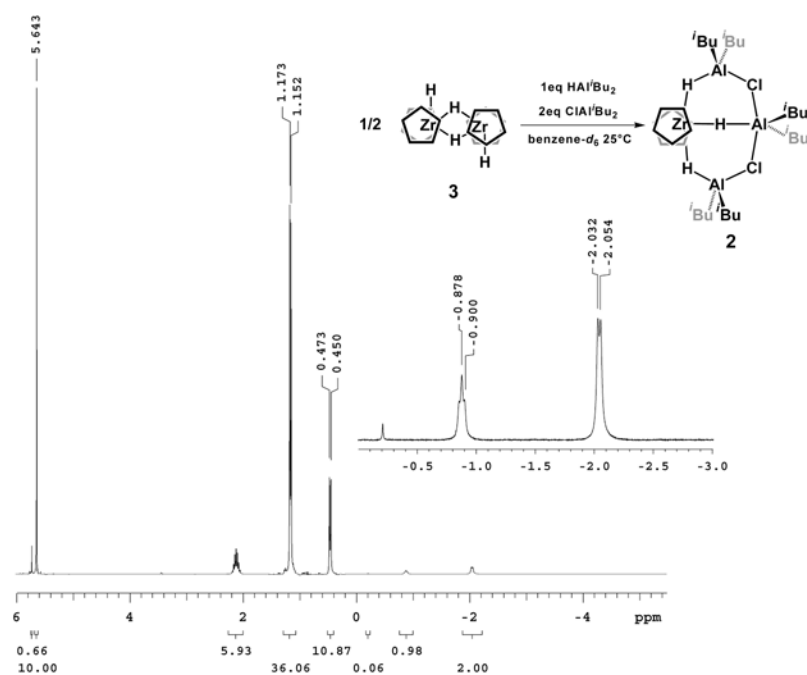


**Figure S3.**  $^1\text{H}$  spectrum of  $(\text{C}_5\text{H}_5)_2\text{Zr}(\mu\text{-H})_3(\text{Al}^i\text{Bu}_2)_3(\mu\text{-H})_3$  in toluene- $d_8$  at  $-60^\circ\text{C}$ .

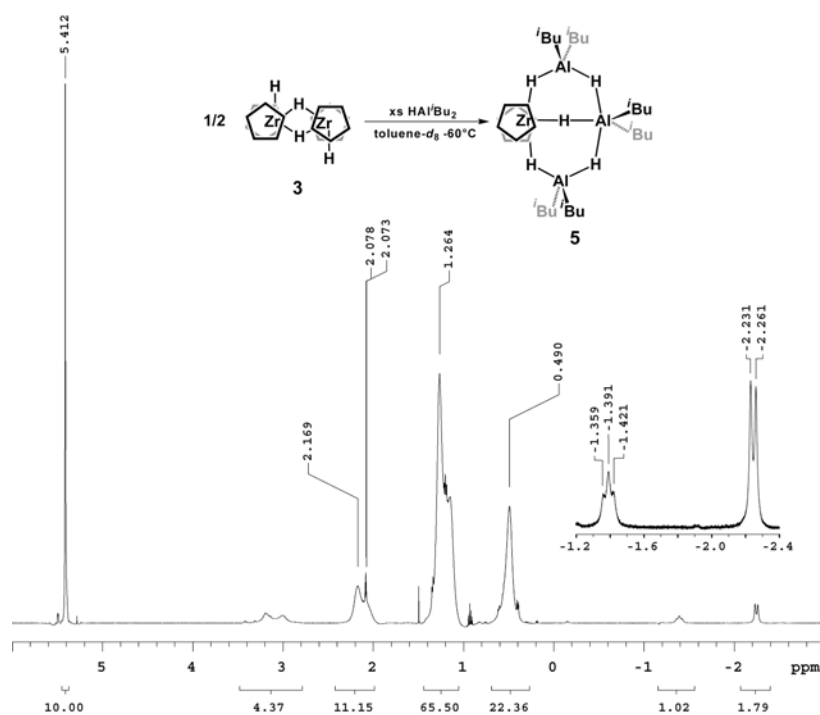


**Figure S4.**  $^1\text{H}$  spectrum of  $(^n\text{Bu-Cp})_2\text{ZrCl}_2$  (6) with 3 equiv.  $\text{HAl}^i\text{Bu}_2$  in benzene- $d_6$  at  $25^\circ\text{C}$

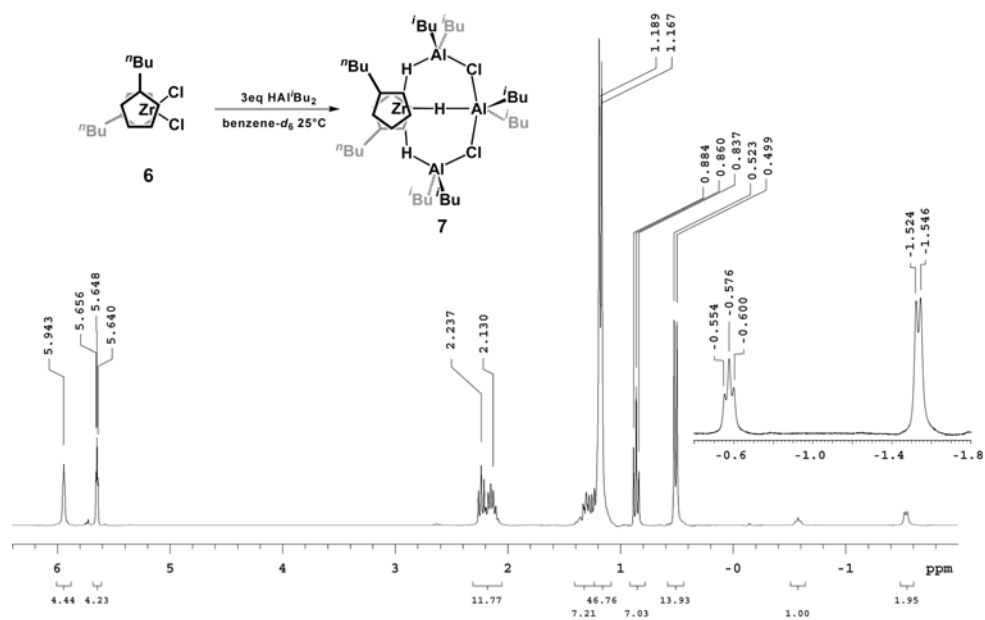


**Figure S5.**  $^1\text{H}$  spectrum of  $(1,2\text{-Me}_2\text{-C}_3\text{H}_3)_2\text{ZrCl}_2$  (**8**) with excess  $\text{HAl}^i\text{Bu}_2$  in benzene- $d_6$  at  $25^\circ\text{C}$ .

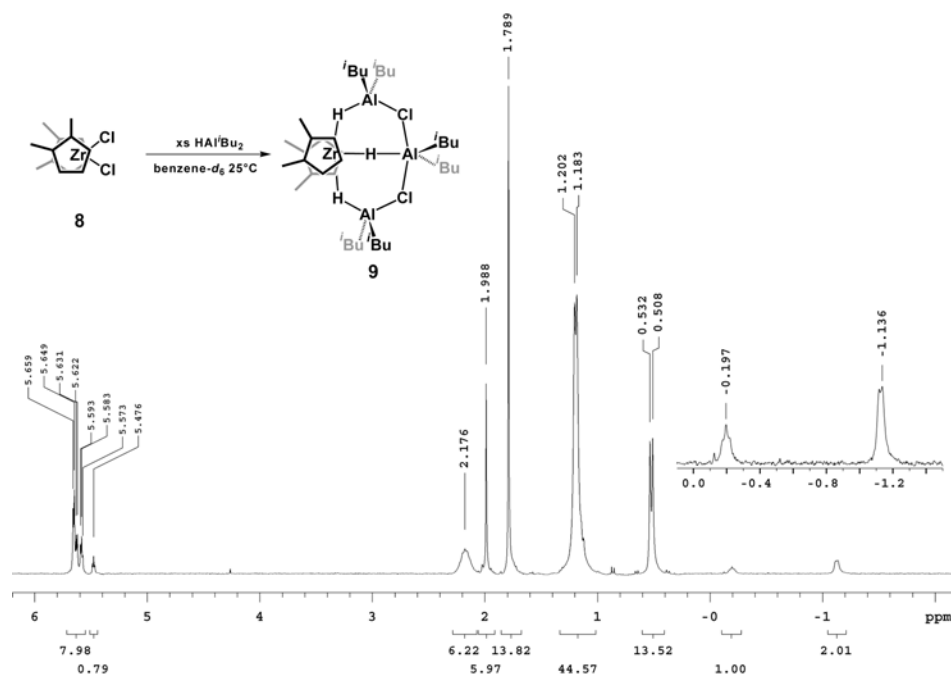


**Figure S6.**  $^1\text{H}$  spectrum of  $(\text{Me}_3\text{Si-C}_5\text{H}_4)_2\text{ZrCl}_2$  (**10**) with 2 equiv.  $\text{HAl}^i\text{Bu}_2$  in toluene- $d_8$  at  $-75^\circ\text{C}$ .

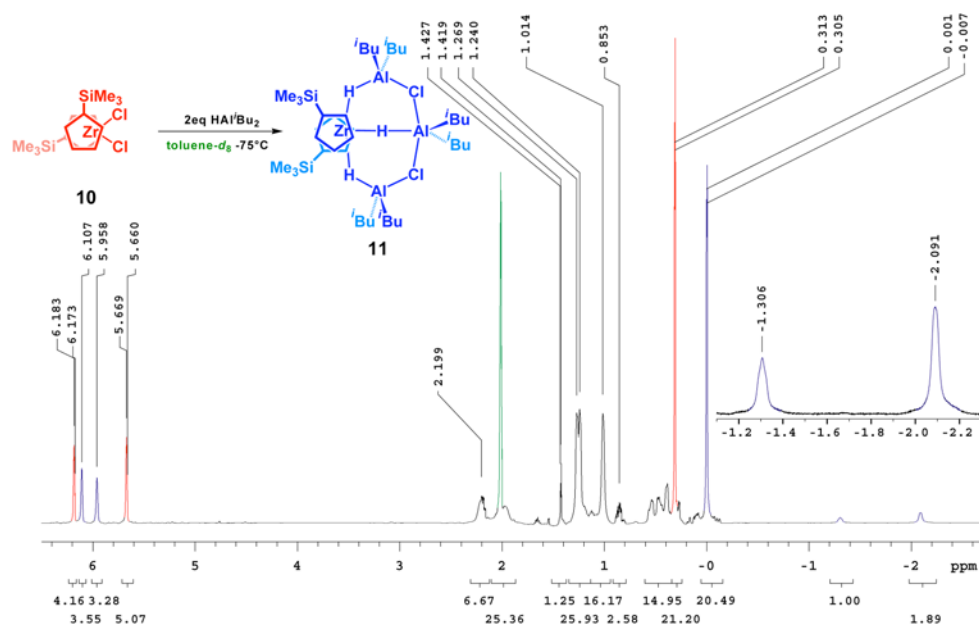


**Figure S7.**  $^1\text{H}$  spectrum of  $(\text{C}_5\text{Me}_5)_2\text{ZrH}_2$  (**13**) with 2 equiv.  $\text{Al}^i\text{Bu}_3$  to give  $(\text{C}_5\text{Me}_5)_2\text{ZrH}^i\text{Bu}$  (**14**) and  $(\text{C}_5\text{Me}_5)_2\text{Zr}^i\text{Bu}_2$  (**15**) in benzene- $d_6$  at 25°C.

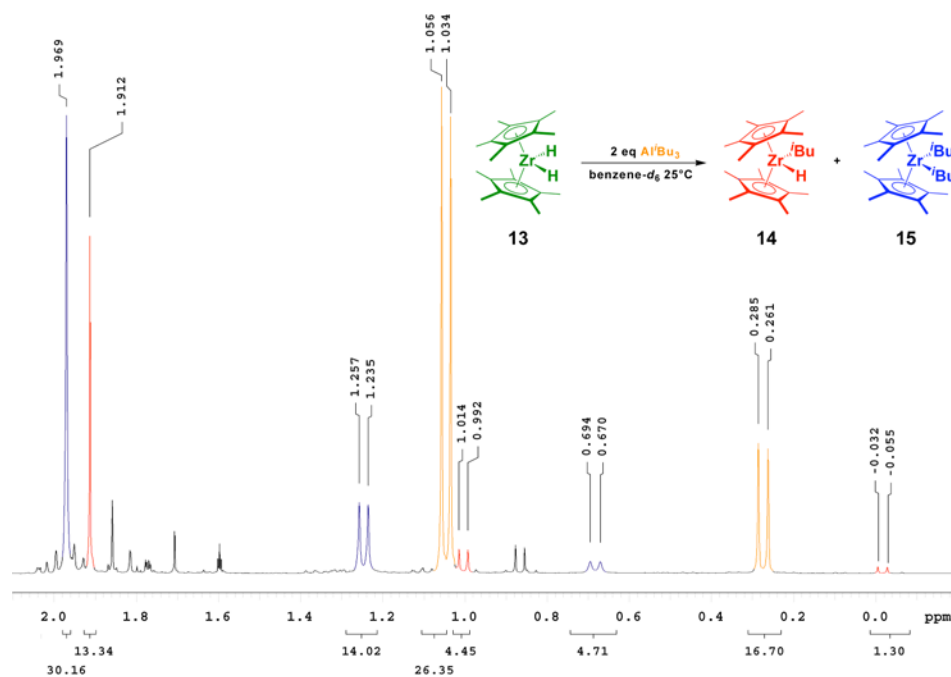


**Figure S8.**  $^1\text{H}$  spectrum of  $(\text{EBI})\text{ZrCl}_2$  (**17**) with 2 equiv.  $\text{HA}^i\text{Bu}_2$  in benzene- $d_6$  at 25°C.

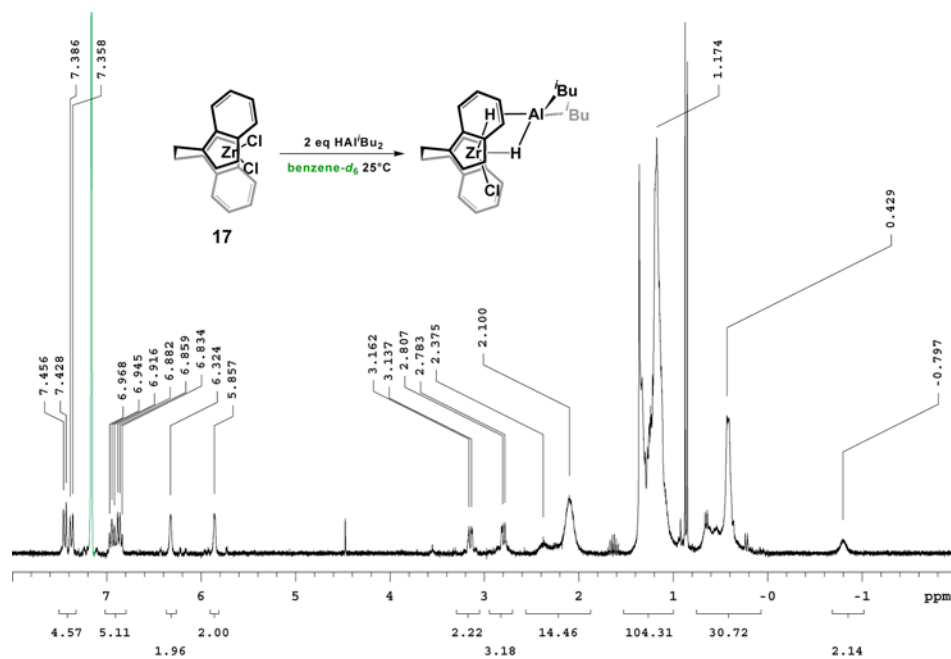


**Figure S9.** (EBTHI)ZrCl<sub>2</sub> (**18**) with 2 equiv. HAl<sup>*i*</sup>Bu<sub>2</sub> in benzene-*d*<sub>6</sub> at 25°C.

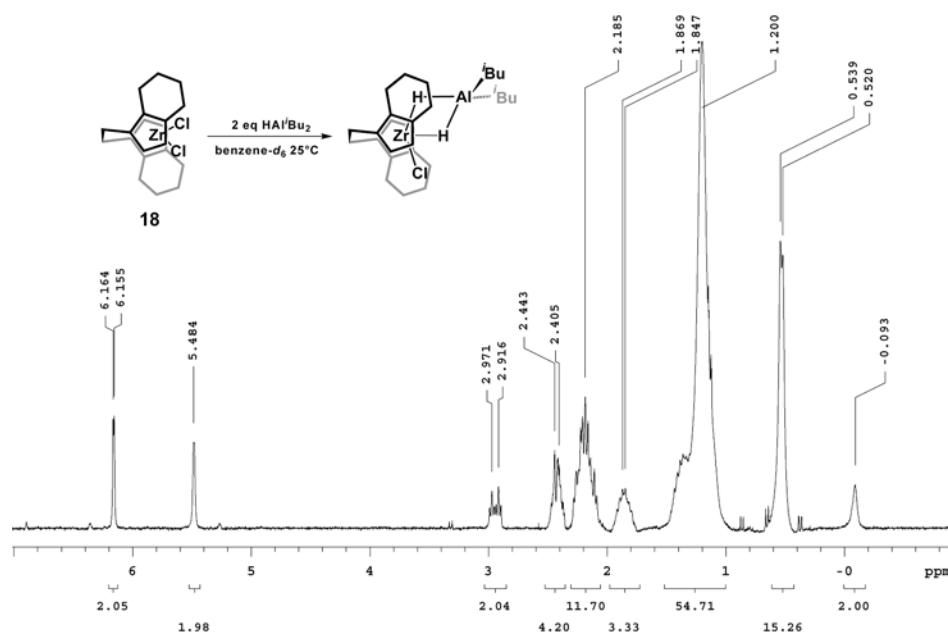


**Figure S10.** <sup>1</sup>H spectrum of Me<sub>2</sub>C(C<sub>5</sub>H<sub>4</sub>)<sub>2</sub>ZrCl<sub>2</sub> (**19**) with excess HAl<sup>*i*</sup>Bu<sub>2</sub> in benzene-*d*<sub>6</sub> at 25°C.

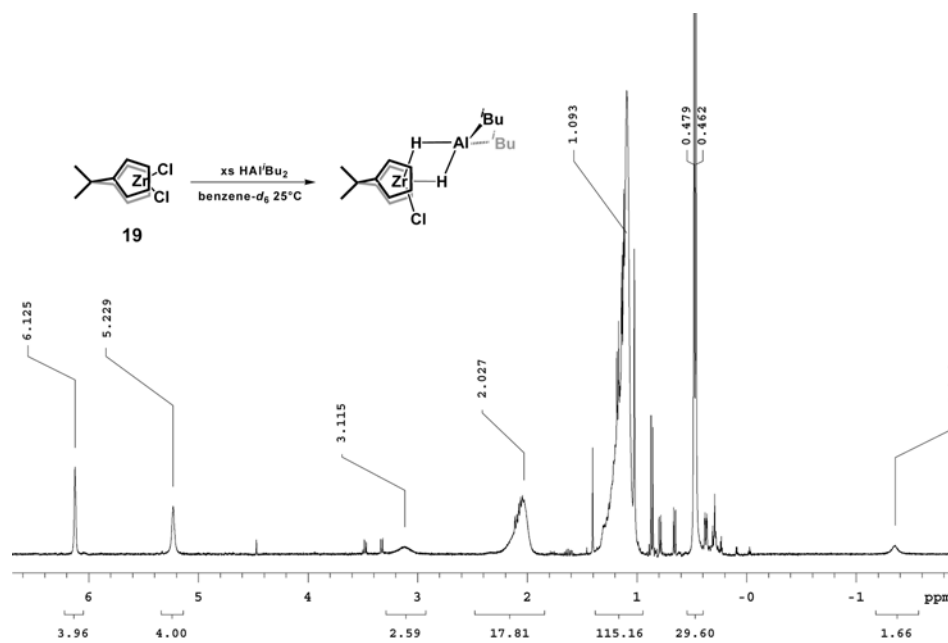


**Figure S11.**  $^1\text{H}$  spectrum of  $\text{Me}_2\text{Si}(\text{C}_5\text{H}_4)_2\text{ZrCl}_2$  (**19**) with 6 equiv.  $\text{HAl}^i\text{Bu}_2$  in benzene- $d_6$  at  $25^\circ\text{C}$ .

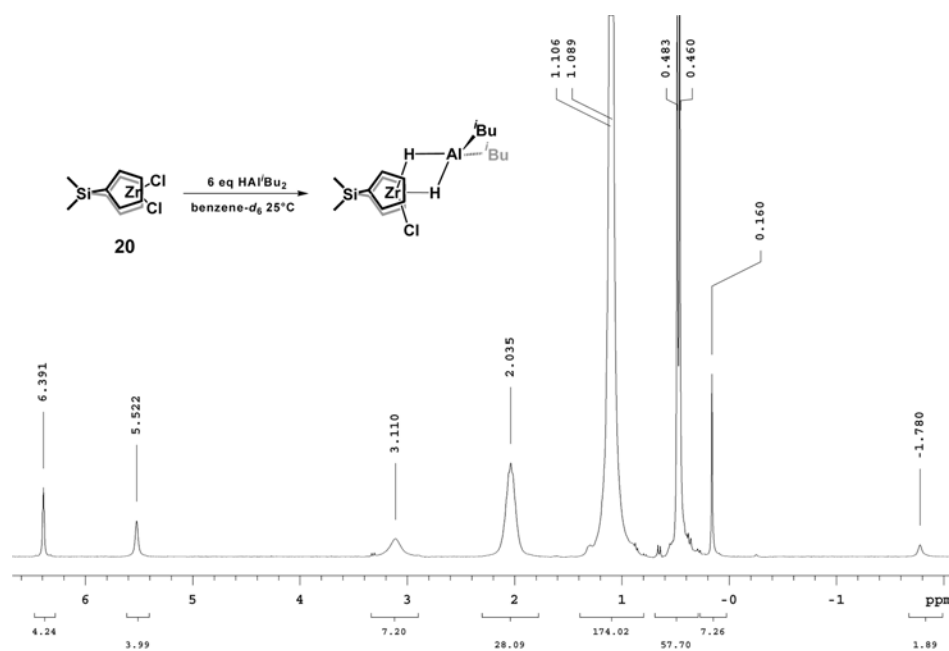


**Figure S12.**  $^1\text{H}$  spectrum of  $\text{Me}_2\text{Si}(2,4\text{-Me}_2\text{-C}_5\text{H}_2)_2\text{ZrCl}_2$  (**21**) with excess  $\text{HAl}^i\text{Bu}_2$  in benzene- $d_6$  at  $25^\circ\text{C}$ .

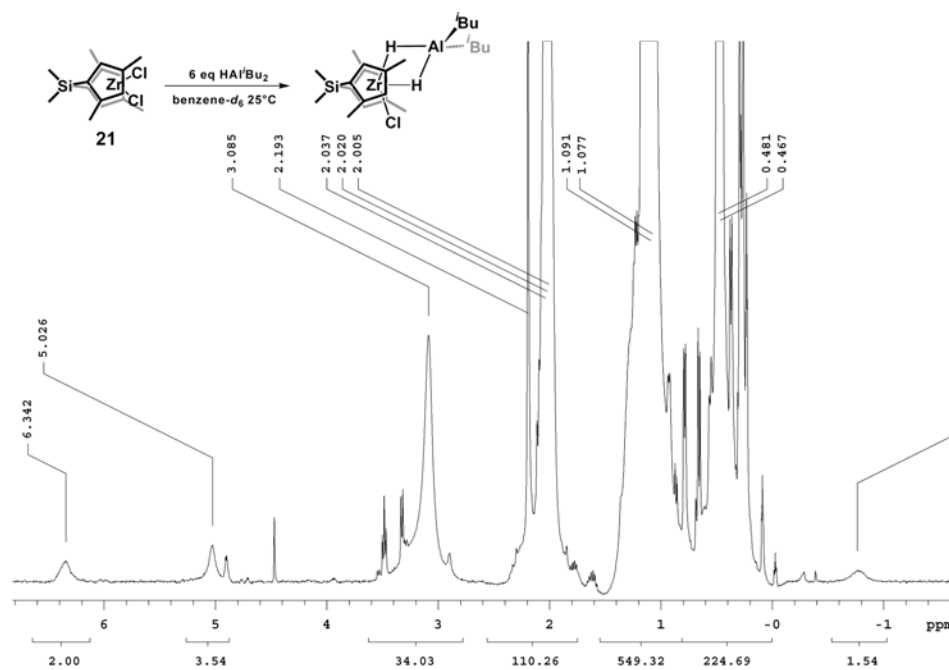




**Figure S13.**  $^1\text{H}$  spectrum of  $(\text{Me}_2\text{Si})_2(\text{C}_5\text{H}_3)_2\text{ZrCl}_2$  (**22**) with 2 equiv.  $\text{HAl}^i\text{Bu}_2$  in toluene- $d_8$  at  $-75^\circ\text{C}$ .

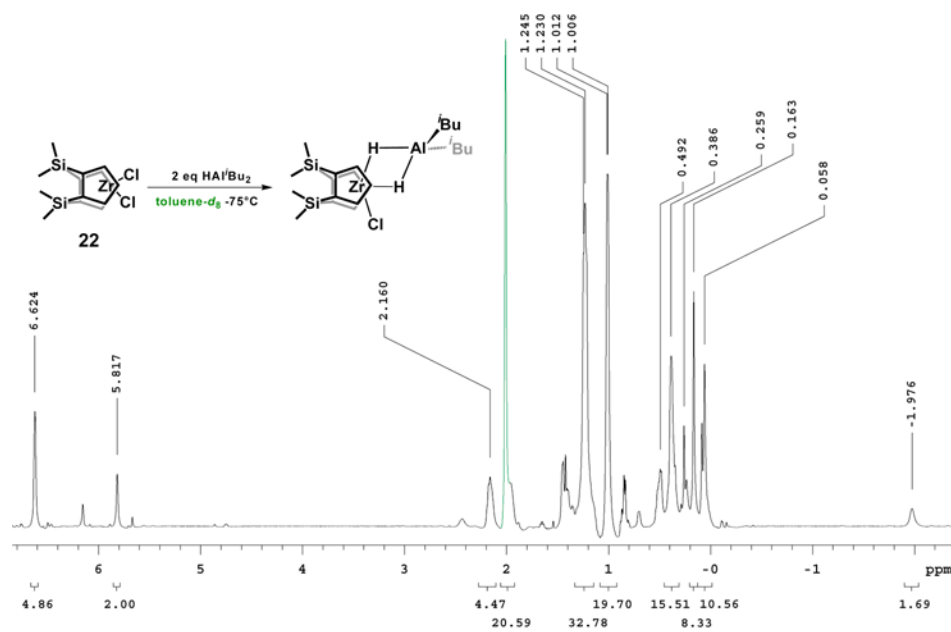


**Figure S14.**  $^1\text{H}$  spectrum of  $(\text{Me}_2\text{Si})_2(2,4\text{-}^i\text{Pr}_2\text{-C}_5\text{H}_3)_2\text{ZrCl}_2$  (**23**) with 2 equiv.  $\text{HAl}^i\text{Bu}_2$  in toluene- $d_8$  at  $-75^\circ\text{C}$ .

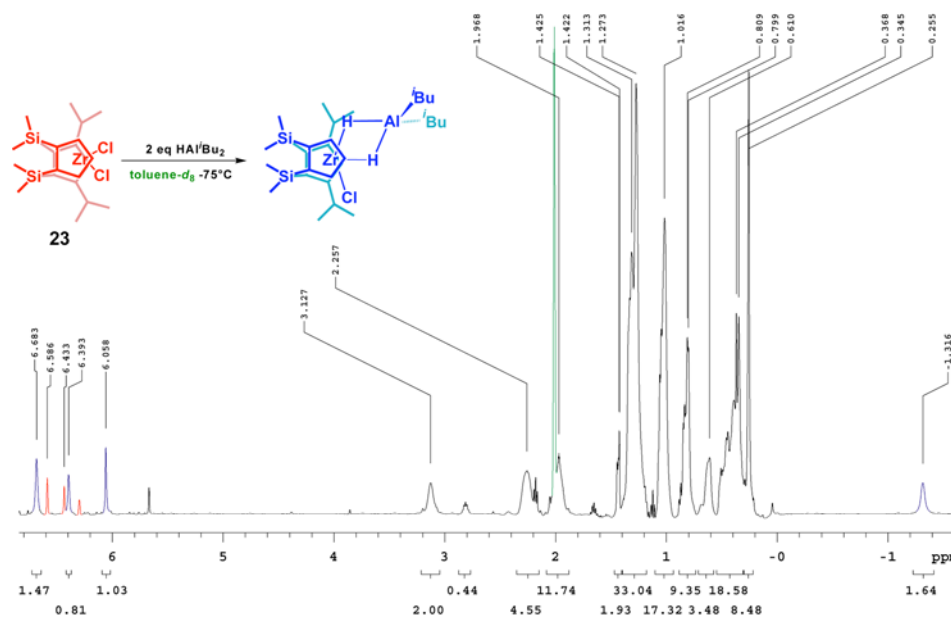


**Figure S15.** gCOSY of (EBTHI)ZrH( $\mu$ -H) $_2$ Al<sup>*i*</sup>Bu<sub>2</sub> (**25**) in toluene-*d*<sub>8</sub> at -75°C.

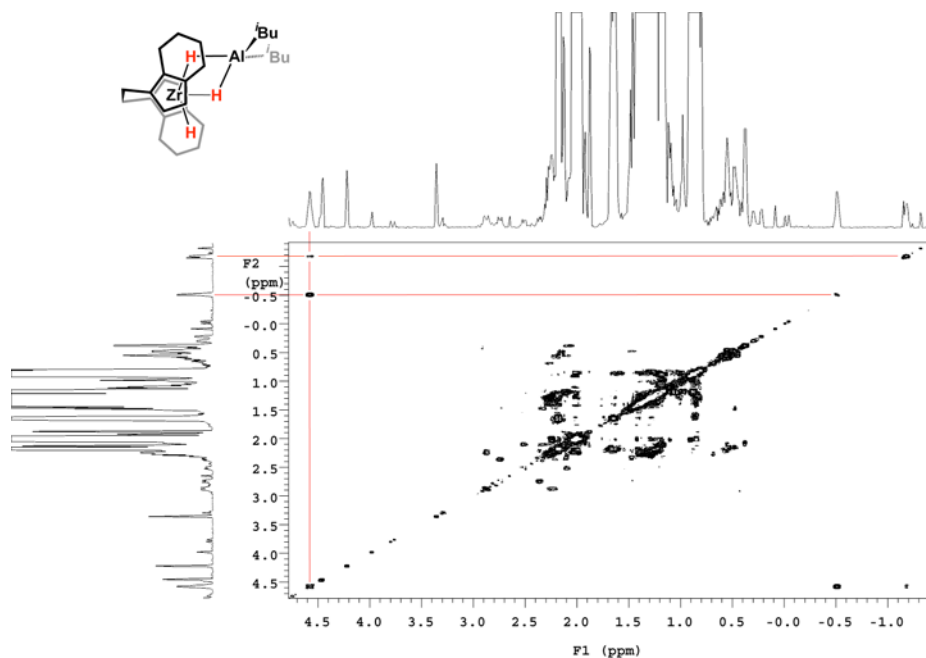


**Figure S16.** <sup>1</sup>H spectrum of ((EBTHI)ZrH( $\mu$ -H))<sub>2</sub> (**24**) with 4 equiv. HAl<sup>*i*</sup>Bu<sub>2</sub> and 2 equiv. ClAl<sup>*i*</sup>Bu<sub>2</sub> in benzene-*d*<sub>6</sub> at 25°C.

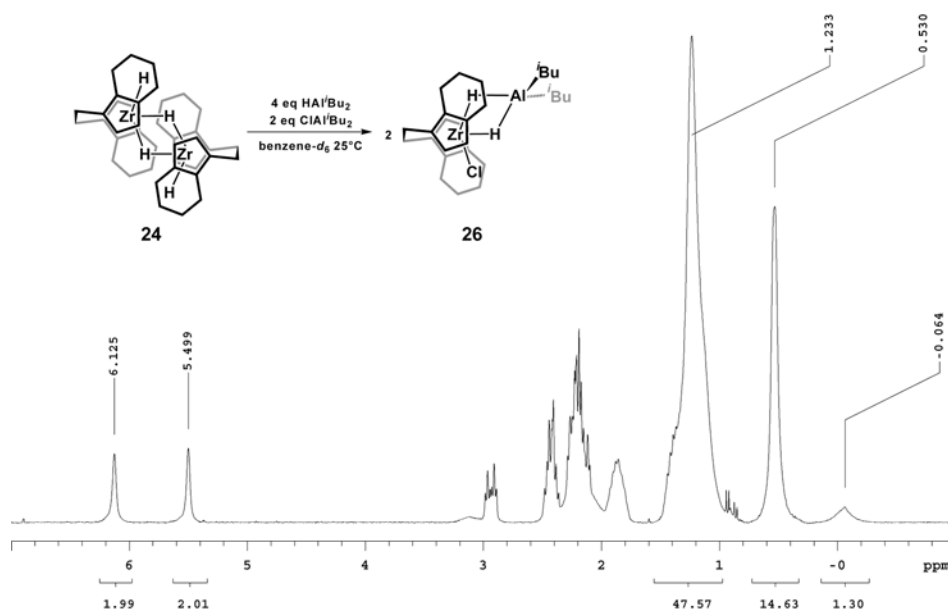


**Figure S17.**  $^1\text{H}$  spectrum of  $((\text{EBTHI})\text{ZrH}(\mu\text{-H})_2)$  (**24**) with 4 equiv.  $\text{HAl}^i\text{Bu}_2$  and 4 equiv.  $\text{ClAl}^i\text{Bu}_2$  in benzene- $d_6$  at 25°C.

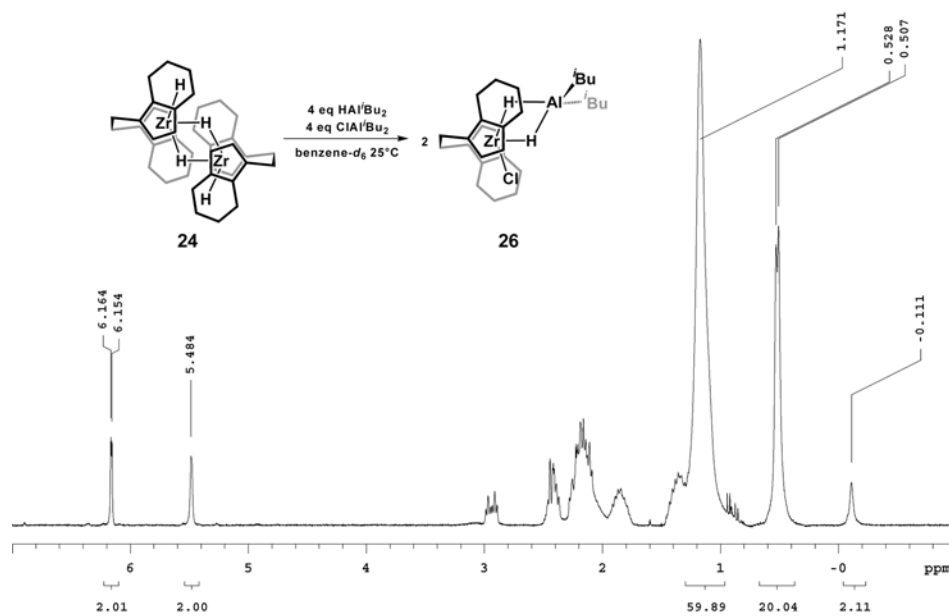


**Figure S18.**  $^1\text{H}$  spectrum of  $\text{rac-Me}_2\text{C}(\text{indenyl})_2\text{ZrCl}_2$  (**27**) with 2 equiv.  $\text{HAl}^i\text{Bu}_2$  in benzene- $d_6$  at 25°C.

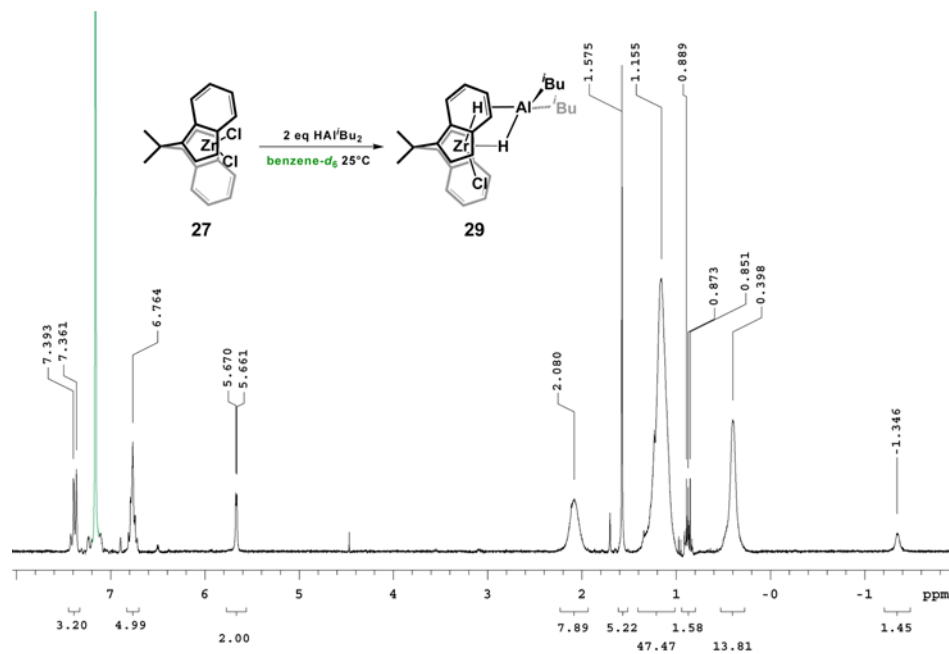


**Figure S19.**  $^1\text{H}$  spectrum of *meso*- $\text{Me}_2\text{C}(\text{indenyl})_2\text{ZrCl}_2$  (**28**) with 2 equiv.  $\text{HAl}^i\text{Bu}_2$  in benzene- $d_6$  at  $25^\circ\text{C}$ .

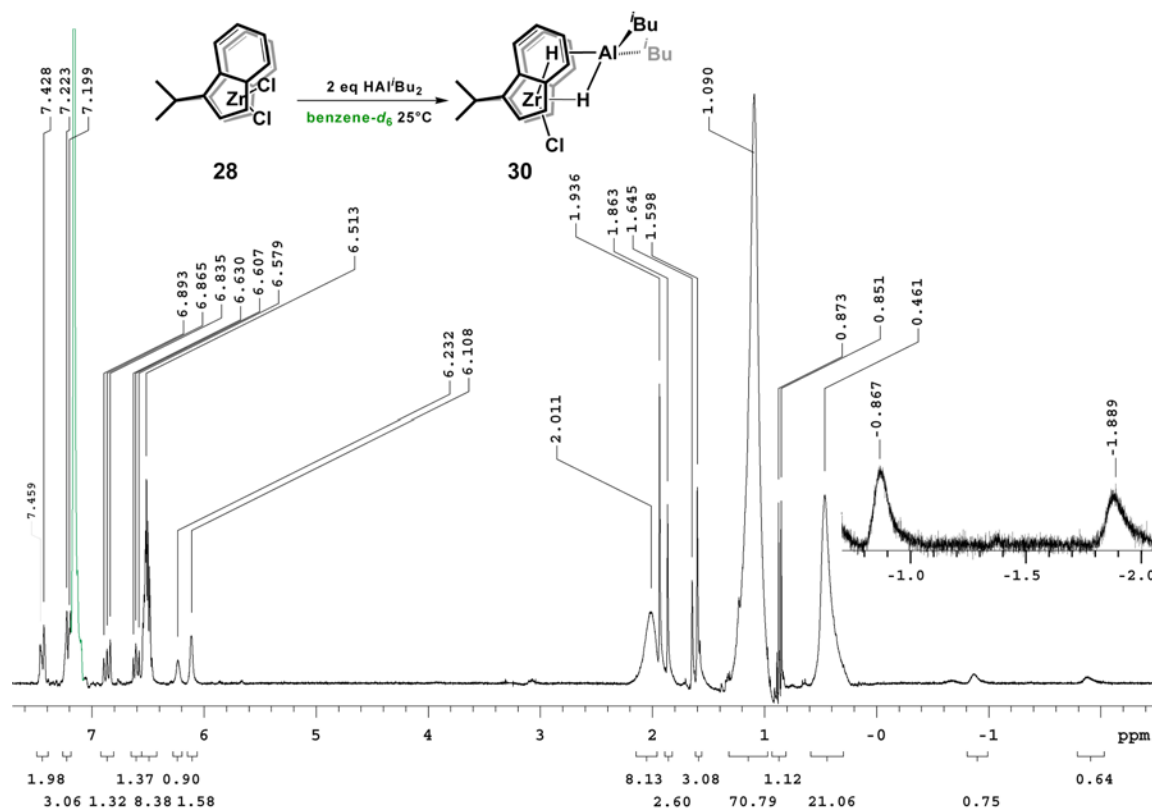


**Figure S20.** gCOSY of *rac*- $\text{Me}_2\text{Si}((2\text{-Me}_3\text{Si-4-Me}_3\text{C-C}_5\text{H}_2)\text{ZrH}(\mu\text{-H})_2\text{Al}^i\text{Bu}_2)$  (**32**) in toluene- $d_8$  at  $-75^\circ\text{C}$

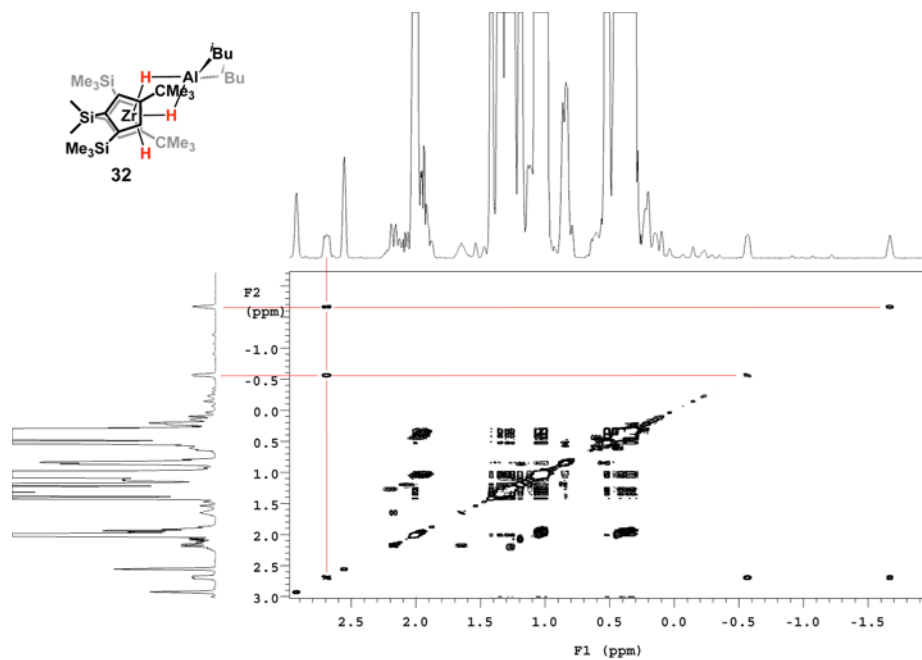


**Figure S21.** noedif of **32** in benzene- $d_6$  at 25°C irradiating the central hydride resonance (**A**) and the terminal unbridged hydride resonance (**B**).

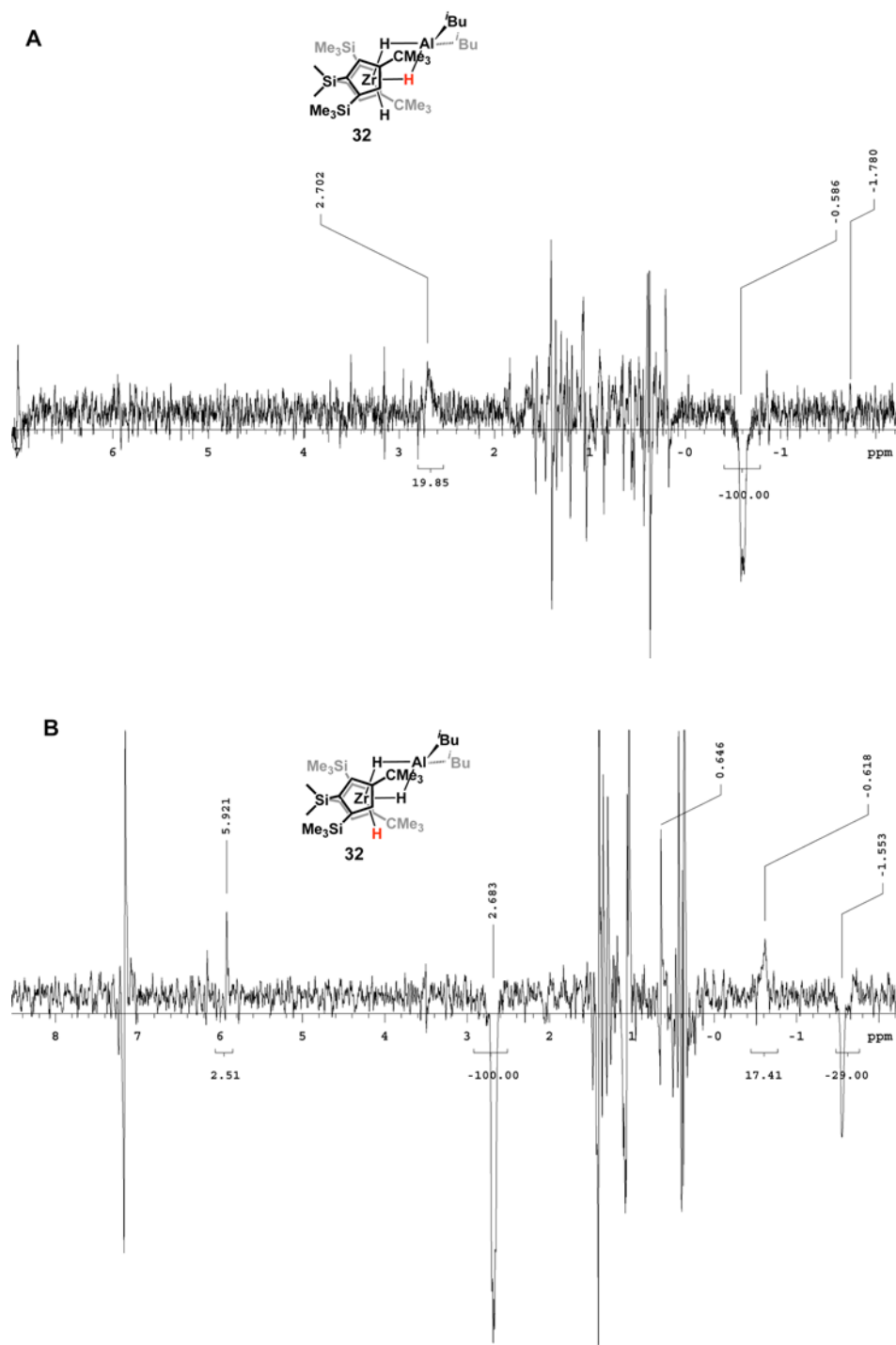


**Figure S22.**  $^1\text{H}$  spectrum of *meso*- $\text{Me}_2\text{Si}(3\text{-Me}_3\text{C-C}_5\text{H}_3)_2\text{ZrCl}_2$  (**33**) with 2 equiv.  $\text{HAl}^i\text{Bu}_2$  in toluene- $d_8$  at  $25^\circ\text{C}$ .

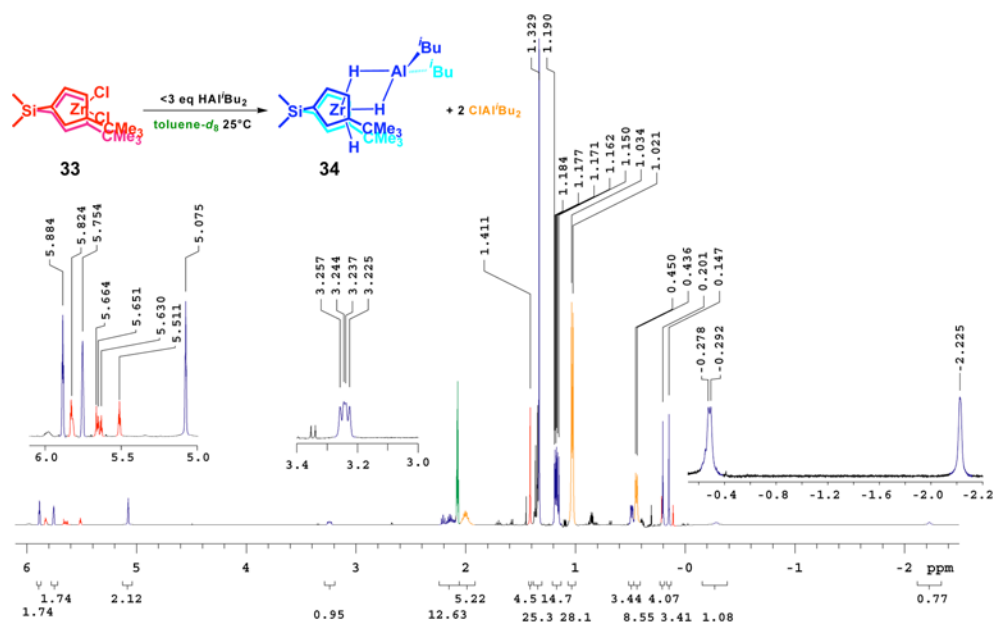


**Figure S23.** gCOSY of **33** with 2 equiv.  $\text{HAl}^i\text{Bu}_2$  in toluene- $d_8$  at  $25^\circ\text{C}$ .

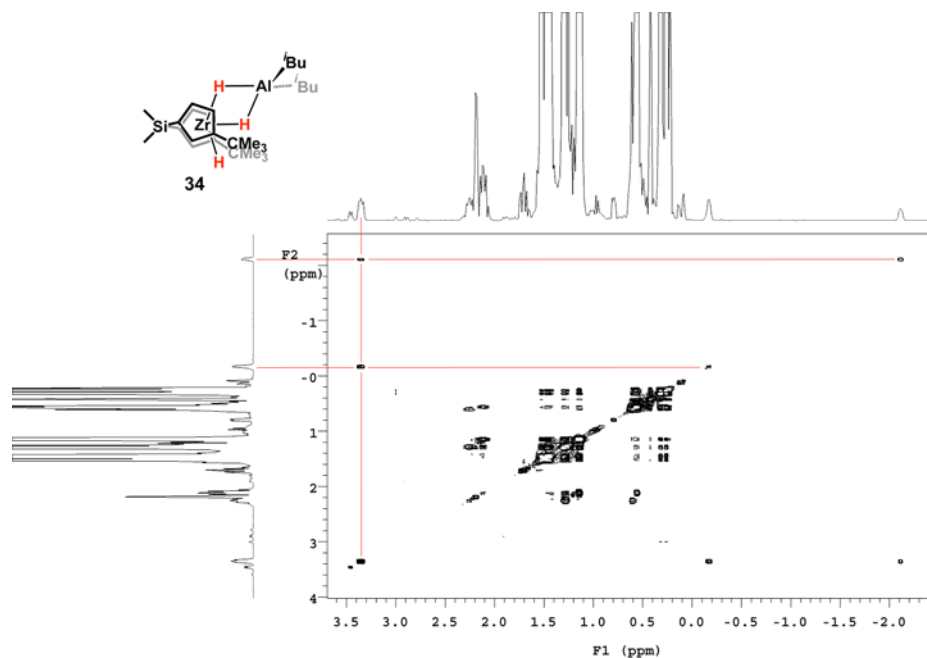


**Figure S24.** noedif of **33** with 3 equiv.  $\text{HAl}^i\text{Bu}_2$  in benzene- $d_6$  at 25°C.

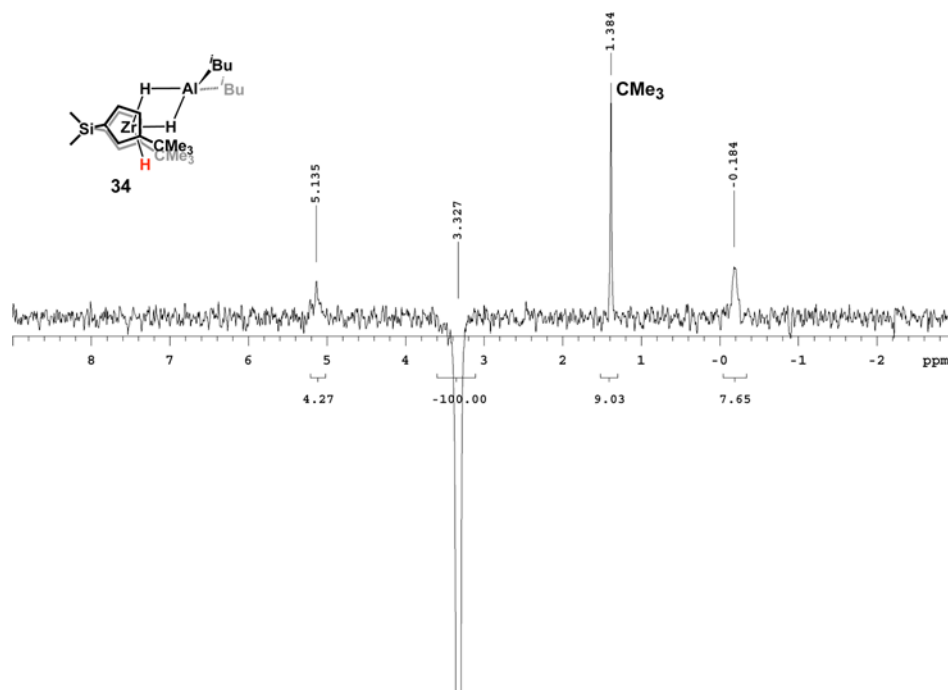


**Figure S25.**  $^1\text{H}$  spectrum of  $\text{H}_4\text{C}_2(\text{C}_5\text{H}_4)_2\text{ZrCl}_2$  (**35**) with 4 equiv.  $\text{HAl}^i\text{Bu}_2$  in toluene- $d_8$  at 0°C.

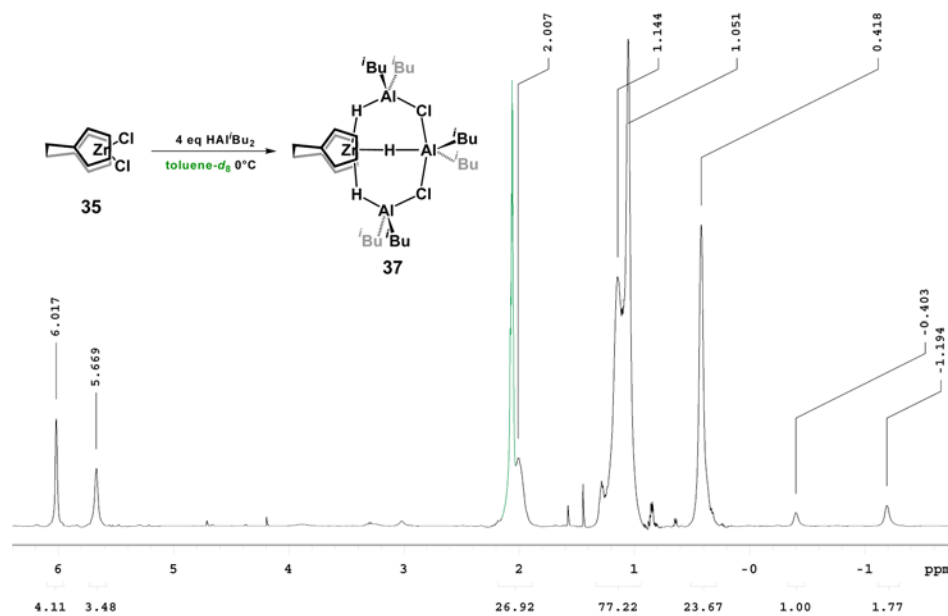


**Figure S26.** NOESY1D of  $\text{Me}_4\text{C}_2(\text{C}_5\text{H}_4)_2\text{ZrCl}_2$  (**36**) with 4 equiv.  $\text{HAl}^i\text{Bu}_2$  in benzene- $d_6$  at 25°C.

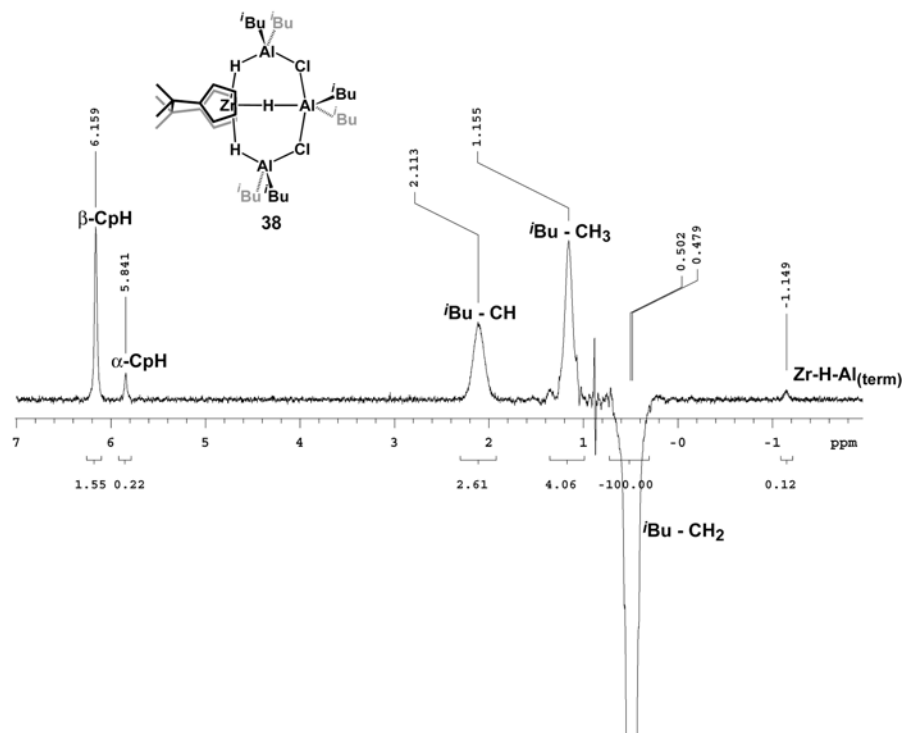
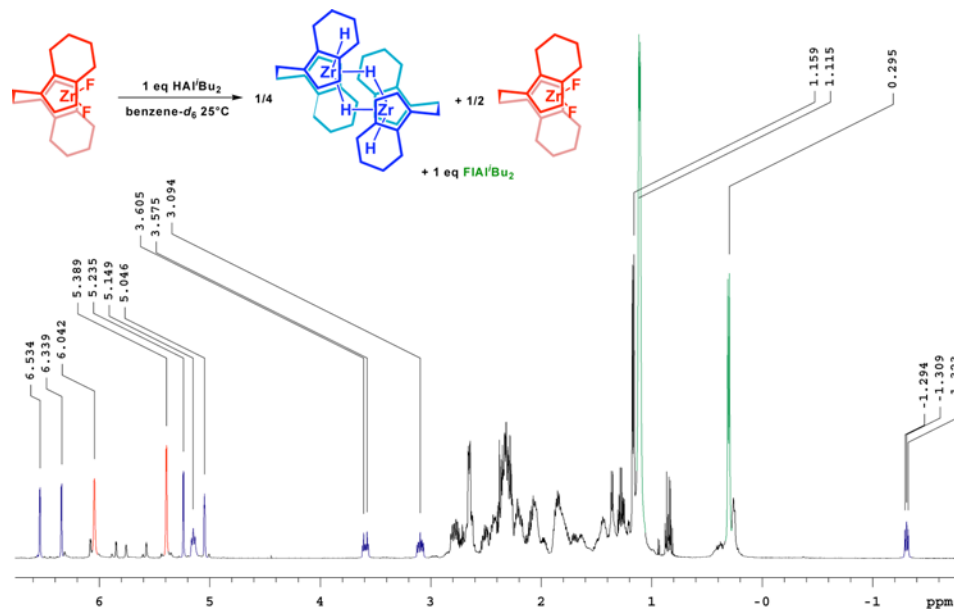


**Figure S27.**  $^1\text{H}$  spectrum of  $(\text{EBTHI})\text{ZrF}_2$  with 1 equiv.  $\text{HAl}^i\text{Bu}_2$  in benzene- $d_6$  at 25°C.





**Appendix S-1.** Analysis of changes in the chemical shift of the  $\text{ZrH}_2$  signal of  $(\text{SBI})\text{ZrCl}(\mu\text{-H})_2\text{Al}^i\text{Bu}_2$  upon addition of  $\text{Al}_2\text{Me}_6$ .

1) Adduct Formation:

Adduct formation of  $(\text{SBI})\text{ZrCl}(\mu\text{-H})_2\text{Al}^i\text{Bu}_2$  with  $\text{Al}_2\text{Me}_6$ , is represented by Equ. 1, with **A** representing the starting complex, **X<sub>2</sub>** the  $\text{AlMe}_3$  dimer and **AX** the adduct:



The equilibrium constant K for this reaction is represented by Equ. 2:

$$K = \frac{[AX]}{[A]\sqrt{[X_2]}} \quad (2)$$

Under conditions of rapid exchange between **A** and **AX** the chemical shift of the resulting signal,  $\delta$ , is the weighted average of the chemical shifts of **A**,  $\delta_A$ , and **AX**,  $\delta_{AX}$  (Equ. 3).

$$\delta = \frac{[A]}{[AX] + [A]} \delta_A + \frac{[AX]}{[AX] + [A]} \delta_{AX} \quad (3)$$

The difference in chemical shift,  $\Delta\delta$ , of the signal at any given concentration of added **X**,  $\delta$ , and that of pure **A** is given by Equ. 4.

$$\Delta\delta = \delta - \delta_A \quad (4)$$

Combining Equ. 3 and Equ. 4 we get:

$$\Delta\delta = \left( \frac{[A]}{[AX] + [A]} - 1 \right) \delta_A + \frac{[AX]}{[AX] + [A]} \delta_{AX} \quad (5)$$

Which simplifies to:

$$\Delta\delta = \frac{[AX]}{[AX] + [A]} (\delta_{AX} - \delta_A) \quad (6)$$

With the maximum change in chemical shift represented as  $\Delta\delta_{\text{max}}$ , we get Equ. 7.

$$\Delta\delta_{\text{max}} = \delta_{AX} - \delta_A \quad (7)$$

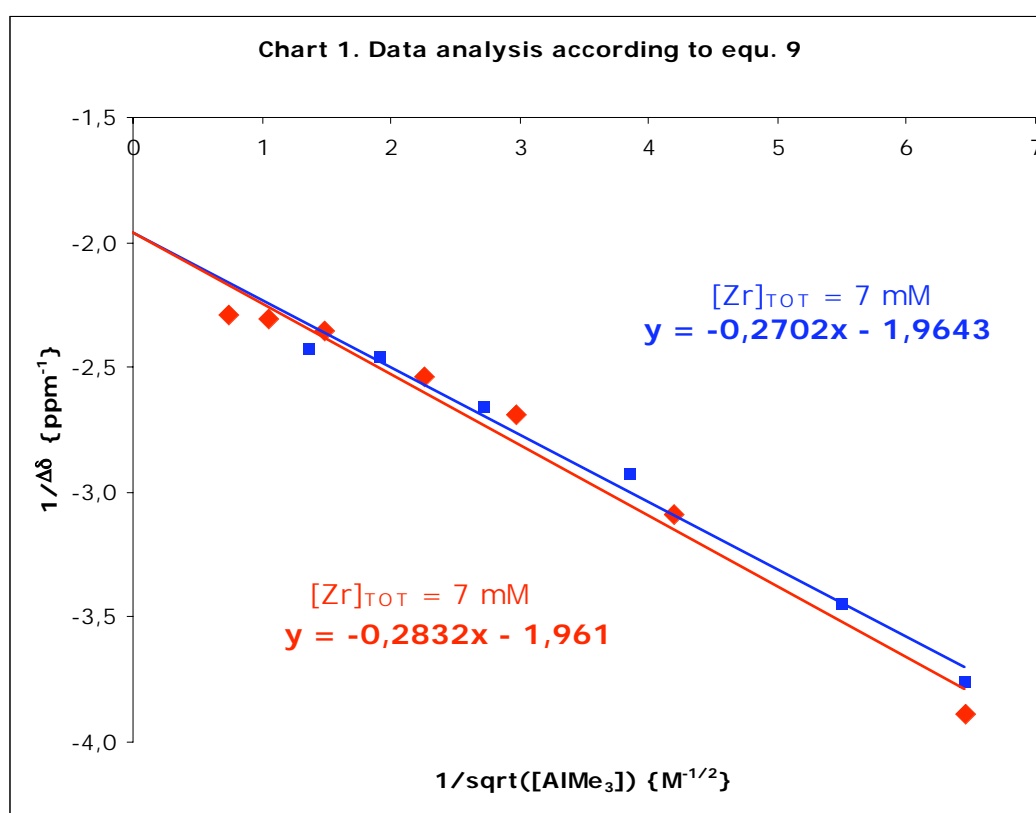
Taking the reciprocal of Equ. 6 and using Equ. 7 gives Equ. 8:

$$\frac{1}{\Delta\delta} = \frac{1}{\Delta\delta_{\text{max}}} + \frac{1}{\Delta\delta_{\text{max}}} \cdot \frac{[A]}{[AX]} \quad (8)$$

Together with the equilibrium constant, Equ. 2, this yields a Benesi-Hildebrand type relation (Equ. 9):

$$\frac{1}{\Delta\delta} = \frac{1}{\Delta\delta_{\max}} + \frac{1}{\Delta\delta_{\max} K \sqrt{[X_2]}} \quad (9)$$

Assuming that K is small, the amount of  $X_2$  added is approximately equal to the amount of  $X_2$  in solution. A plot of the reciprocal of the change in chemical shift against the reciprocal of the square root of the concentration of  $Al_2Me_6$  added should thus be linear, with a slope of  $1/K$  and a y-axis intercept of  $1/\delta_{AX}$ , neither of which should depend on  $[Zr]_{TOT}$ .



The data plotted in Chart 1 according to Equation 9 approximate this requirement. Some curvature of the data in Chart 1 might originate from a partial dissociation of  $Al_2Me_6$  to  $AlMe_3$  in dilute solutions and/or from the fact that the most concentrated solutions of  $Al_2Me_6$  contain up to 20 volume percent  $Al_2Me_6$ , such that these solution can no longer be considered to be ideal solutions of  $Al_2Me_6$  in benzene. Nevertheless, the values of  $1/\delta_{\max}$  and of  $1/K$  derived from the data for  $[Zr] = 7$  mM and from those for  $[Zr] = 28$  mM are indistinguishable within their error

margins. Our data are thus compatible with the view that the change in chemical shift of the  $\text{ZrH}_2$  signal upon addition of  $\text{Al}_2\text{Me}_6$  to a solution of  $(\text{SBI})\text{Zr}(\text{Cl})(\mu\text{-H})_2\text{Al}^i\text{Bu}_2$  is due to formation of an adduct, e.g. of the type  $(\text{SBI})\text{Zr}(\text{Cl}\cdots\text{AlMe}_3)(\mu\text{-H})_2\text{AlR}_2$ , with  $\text{R} = {}^i\text{Bu}$  and/or  $\text{Me}$ .

## 2) Exchange Reaction:

The reaction of  $(\text{SBI})\text{ZrCl}(\mu\text{-H})_2\text{Al}^i\text{Bu}_2$  to exchange either the Zr-bound Cl or an Al-bound  ${}^i\text{Bu}$  with one of the methyl groups of  $\text{Al}_2\text{Me}_6$ , to yield  $\text{Al}_2\text{Me}_5\text{X}$  where  $\text{X} = \text{Cl}$  or  ${}^i\text{Bu}$ , is represented by Equ. 10, with **A** representing the starting  $\text{ZrClH}_2$  complex, **X<sub>2</sub>** the  $\text{AlMe}_3$  dimer, **B** the exchange product and **Y** the  $\text{Al}_2\text{Me}_5\text{X}$  product:



The equilibrium constant K for this reaction is represented by Equ. 2:

$$K = \frac{[\text{B}][\text{Y}]}{[\text{A}][\text{X}_2]} \quad (11)$$

We can use the same derivation as for Equation 8, except  $[\text{AX}]$  is now replaced by  $[\text{B}]$ .

$$\frac{1}{\Delta\delta} = \frac{1}{\Delta\delta_{\max}} + \frac{1}{\Delta\delta_{\max}} \cdot \frac{[\text{A}]}{[\text{B}]} \quad (12)$$

Using the equilibrium constant, Equ. 11, this yields a Benesi-Hildebrand type relation (Equ. 13):

$$\frac{1}{\Delta\delta} = \frac{1}{\Delta\delta_{\max}} + \frac{1}{\Delta\delta_{\max}} \cdot \frac{[\text{Y}]}{K[\text{X}_2]} \quad (13)$$

Since we are adding **X<sub>2</sub>** to **A**,  $[\text{Y}]$  is equal to  $[\text{B}]$ , yielding:

$$\frac{1}{\Delta\delta} = \frac{1}{\Delta\delta_{\max}} + \frac{1}{\Delta\delta_{\max}} \cdot \frac{[\text{B}]}{K[\text{X}_2]} \quad (14)$$

Rearranging to give a  $y = mx+b$  format gives:

$$\frac{1}{\Delta\delta} = \left( \frac{[\text{B}]}{\Delta\delta_{\max} K} \right) \cdot \frac{1}{[\text{X}_2]} + \frac{1}{\Delta\delta_{\max}} \quad (15)$$

Alternatively Equ. 14 can be modified by using the following relationship which is derived by combining Equ. 3, 4 and 7:

$$\Delta\delta = \Delta\delta_{\max} \frac{[\text{B}]}{[\text{A}] + [\text{B}]} \quad (16)$$

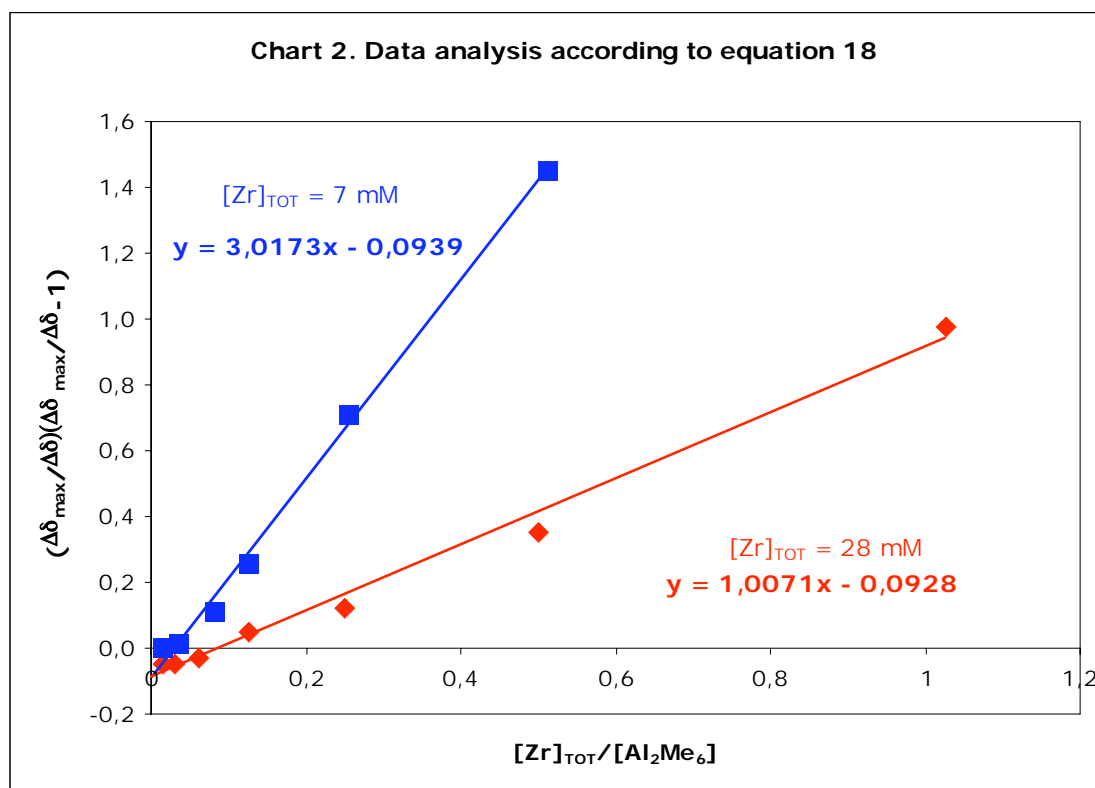
Solving for  $[\text{B}]$  and substituting into Equation 14 gives:

$$\frac{1}{\Delta\delta} = \frac{1}{\Delta\delta_{\max}} + \frac{\Delta\delta}{\Delta\delta_{\max}} \cdot \frac{[A] + [B]}{\Delta\delta_{\max} K [X_2]} \quad (17)$$

With  $[A] + [B] = [\text{Zr}]_{\text{TOT}}$  and  $[X_2] = [\text{Al}_2\text{Me}_6]$ , equation 17 can be rearranged to:

$$\left( \frac{\Delta\delta_{\max}}{\Delta\delta} - 1 \right) \frac{\Delta\delta_{\max}}{\Delta\delta} = \frac{[\text{Zr}]_{\text{TOT}}}{K \cdot [\text{Al}_2\text{Me}_6]} \quad (18)$$

The value of  $\Delta\delta_{\max}$  can be estimated from the chemical shift at the highest concentrations of  $\text{Al}_2\text{Me}_6$  or from the plot in Chart 1. Assuming that  $K$  is small, the amount of  $\text{Al}_2\text{Me}_6$  added is approximately equal to the amount of  $\text{Al}_2\text{Me}_6$  in solution. Therefore, a plot of the left side of Equ.18 against  $[\text{Zr}]_{\text{TOT}}/[\text{Al}_2\text{Me}_6]$  should give a straight line going through the origin, with a slope of  $1/K$ , which should thus be independent of  $[\text{Zr}]_{\text{TOT}}$ .



Inspection of such a plot (Chart 2) shows that the data do not meet this requirement. Instead, the slope of the data for  $[\text{Zr}]_{\text{tot}} = 7 \text{ mM}$  is about three times larger than that of the data for  $[\text{Zr}]_{\text{tot}} = 28 \text{ mM}$ . The change in chemical shift of the  $\text{ZrH}_2$  signal upon addition of  $\text{Al}_2\text{Me}_6$  to a solution of  $(\text{SBI})\text{Zr}(\text{Cl})(\mu\text{-H})_2\text{Al}^i\text{Bu}_2$  can thus **not** be due to an exchange reaction, e.g. of the Cl against a Me ligand.